

Research Article

Int J Energy Studies 2024; 9(3): 381-397

DOI: 10.58559/ijes.1531980

Received : 12 Aug 2024

Revised : 23 Aug 2024

Accepted : 26 Aug 2024

## Comprehensive modeling of solid oxide electrolyzer cells for H<sub>2</sub>O and CO<sub>2</sub> co-electrolysis

Berre Kumuk\*

\*Automotive Technologies Program, Iskenderun Vocational School of Higher Education, Iskenderun Technical University, Hatay, Turkey, ORCID: 0000-0001-7953-0167

(\*Corresponding Author: [berre.kumuk@iste.edu.tr](mailto:berre.kumuk@iste.edu.tr))

### Highlights

- Anode-supported SOECs outperformed cathode-supported and electrolyte-supported counterparts.
- Increasing operating temperature was identified as a key factor in enhancing SOEC performance.
- Comparison of co-flow and cross-flow configurations revealed minor differences in performance.

**You can cite this article as:** Kumuk B. Comprehensive modeling of solid oxide electrolyzer cells for H<sub>2</sub>O and CO<sub>2</sub> co-electrolysis. Int J Energy Studies 2024; 9(3): 381-397.

### ABSTRACT

In this study, a 2D model of Solid Oxide Electrolysis Cells (SOECs) was developed to evaluate their performance in CO<sub>2</sub> and H<sub>2</sub>O co-electrolysis. The numerical results were rigorously validated against prior studies, demonstrating high consistency. The investigation focused on understanding the influence of various factors such as support type and operating temperature on SOEC performance. Analysis of polarization and performance curves revealed that anode-supported and cathode-supported SOECs exhibited similar characteristics, while electrolyte-supported SOECs displayed lower performance due to inadequate conductivity and increased electrolyte thickness. At 1.6 V, the average current density for cathode-supported SOEC was approximately 2.3679 A/cm<sup>2</sup>, slightly lower than that of anode-supported SOEC, which was approximately 2.3879 A/cm<sup>2</sup>. Moreover, at an average current density of around 5.30 A/cm<sup>2</sup>, the cathode-supported SOEC yielded an average power density of 10 W/cm<sup>2</sup>, while the anode-supported SOEC achieved 10.1 W/cm<sup>2</sup>. Furthermore, increasing temperature was found to enhance SOEC performance by promoting more efficient chemical reactions, reducing resistance, and improving gas production rates during electrolysis of H<sub>2</sub>O and CO<sub>2</sub>. However, careful consideration of optimal operating temperatures is essential to ensure cell durability and material lifespan. Moreover, comparing co-flow and cross-flow configurations highlighted minor differences in performance, with co-flow demonstrating slightly lower average current density but comparable power density at 1.6 V. Co-flow configuration was favored for its homogeneous operation, facilitating efficient gas mixing and diffusion, while counter-flow configurations may introduce heterogeneity, potentially affecting overall performance. Overall, this study provides valuable insights into optimizing SOEC performance and efficiency, emphasizing the importance of support type, operating temperature, and flow configuration in achieving optimal performance for CO<sub>2</sub> and H<sub>2</sub>O co-electrolysis applications.

**Keywords:** Solid oxide electrolyzer, CO<sub>2</sub> co-electrolysis, H<sub>2</sub>O co-electrolysis, Numerical modeling

## 1. INTRODUCTION

Solid oxide electrolyzer cells (SOECs) are high-efficiency and environmentally friendly technology that plays a significant role in energy conversion. These electrochemical devices can convert electrical energy into chemical energy or vice versa, making them highly versatile for various applications such as energy storage and integration of renewable energy. SOECs operate at high temperatures (typically between 500 to 1000°C) and utilize solid oxide electrolytes (usually stabilized zirconia with yttrium or cerium). This high temperature allows SOECs to perform thermochemical conversions, enabling the production of energy-dense fuels (such as hydrogen or synthetic fuels) [1,2].

Key advantages of SOECs include high energy efficiency, long lifespan, low carbon emissions, and fuel flexibility. These features enable the use of SOECs across a wide range of applications, from energy storage systems to electrochemical conversion of industrial gases. Particularly in combating fluctuations in renewable energy sources and reducing carbon emissions, SOECs can play a crucial role in the production of hydrogen and synthetic fuels, the synthesis of carbon-neutral products in industrial processes, and even steel production. Therefore, SOECs are a critical technology in achieving sustainable energy conversion and carbon reduction goals [3–6].

Carbon dioxide (CO<sub>2</sub>) electrolysis in SOECs presents several significant advantages and holds paramount importance in the realm of sustainable energy technologies. One key advantage lies in its ability to convert CO<sub>2</sub>, a greenhouse gas linked to climate change, into valuable and renewable fuels such as carbon monoxide (CO) or syngas, which can be further processed into a variety of hydrocarbons or utilized as feedstock for other chemical processes. By harnessing renewable electricity from sources like solar or wind power, CO<sub>2</sub> electrolysis in SOECs offers a pathway for carbon-neutral or even carbon-negative fuel production, thereby contributing to efforts aimed at mitigating climate change and reducing reliance on fossil fuels. Moreover, the integration of CO<sub>2</sub> electrolysis with renewable energy sources enables the utilization of intermittent energy surpluses, enhancing grid stability and promoting the efficient utilization of renewable resources. Overall, the ability of SOECs to perform CO<sub>2</sub> electrolysis represents a crucial step towards achieving a sustainable energy future by simultaneously addressing environmental concerns and advancing the development of renewable energy technologies [7–10].

Xu et al. investigated the numerical effects of CH<sub>4</sub>-assisted CO<sub>2</sub>/H<sub>2</sub>O co-electrolysis in SOECs, aiming at simultaneous energy storage and CO<sub>2</sub> utilization. The study demonstrates that CH<sub>4</sub> assistance effectively reduces the equilibrium potential of SOEC, thereby significantly lowering electrical power consumption during co-electrolysis. Results indicate that CH<sub>4</sub>-assisted SOEC performance improves notably with increasing temperature, attributed to enhanced reaction kinetics. Unlike conventional SOECs, CH<sub>4</sub>-assisted SOEC performance exhibits sensitivity to anode gas flow rates, achieving peak current density at specific flow rates. These findings offer insights for optimizing SOEC design towards high-performance energy storage applications [11].

Song et al. demonstrated stable and high-performance pure CO<sub>2</sub> electrolysis over Ni/YSZ cathodes at 700°C without the need for a reductive gas through experimental and theoretical analysis. In-situ electroreduction of the cathode's nickel oxide layer and theoretical calculations support the finding that electrolysis voltage facilitates continuous electron flow across the cathode, mitigating nickel oxidation. Moreover, the electrochemical performance of pure CO<sub>2</sub> electrolysis over Ni/YSZ cathodes surpasses that of a reductive gas, highlighting the potential for improved stability and efficiency in CO<sub>2</sub> electrolysis systems [12].

Wang et al. employed a 3D continuum model to analyze the dynamic behavior and control strategy of a 3-kW 40-cell planar SOEC stack during CO<sub>2</sub> and H<sub>2</sub>O co-electrolysis. The study focused on assessing the dynamic responses of stack power, current density, H<sub>2</sub>/CO ratio, and temperature under variable wind power input. Fluctuations in wind power input cause temperature variations in the SOEC stack, highlighting the importance of temperature control. Two scenarios with voltage step changes are investigated to predict temperature control using excess air ratio variation. The study revealed that adjusting the excess air ratio effectively controls temperature fluctuations induced by wind power variations [13].

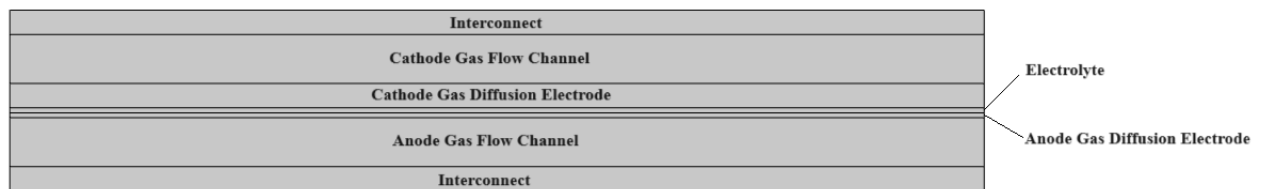
Luo et al. explored direct power-to-methane conversion in SOECs with low inlet H<sub>2</sub> content. Results in a decreased ratio of H<sub>2</sub> consumption to total energy consumption (41%) and an increased energy-to-CH<sub>4</sub> efficiency (53%) [14].

Mahmood et al. focused on enhancing the performance of Ni-cermet-supported SOECs for CO<sub>2</sub>/H<sub>2</sub>O co-electrolysis by reducing cathodic polarization resistances through thickness reduction. Electrochemical measurements and impedance spectroscopy are conducted at temperatures ranging from 750 to 850°C for various reactant gas compositions. Results showed that decreasing cathode thickness reduces concentration polarization, improving reactant gas diffusion and overall SOEC performance. Additionally, increasing the CO<sub>2</sub> mole fraction in the feed yields similar improvements. These findings highlight the potential for optimizing cell design to enhance gaseous transport and SOEC performance for CO<sub>2</sub>/H<sub>2</sub>O reduction [15].

In this study, the performance of a two-dimensional SOEC for CO<sub>2</sub> electrolysis has been investigated. The research extensively examines the type of support structure, temperature, and flow direction. The main objective of this study is to establish a guide for determining the optimal conditions for producing SOECs for experimental studies.

## 2. MATHEMATICAL MODELLING

The 2D SOEC model used in the study is illustrated in Figure 1. In the study, a mixture of H<sub>2</sub>O, CO<sub>2</sub>, H<sub>2</sub>, CO, and CH<sub>4</sub> is supplied from the cathode electrode, while air is supported by the anode electrode. The reactions occurring in the anode and cathode electrodes are depicted by Equations 1-3.



**Figure 1.** 2D SOEC model



Table 1 shows that the values of parameters used in the 2D SOEC model.

**Table 1.** Input parameters used in the model

Parameter	Value
Electrode porosity	0.4
Electrolyte volume fraction	0.4
Electrode tortuosity	3
Gas flow channel height	1 mm
Interconnect thickness	500 μm

SOEC length	20 mm
<i>Thickness for cathode-supported SOEC</i>	
Cathode thickness	400 μm
Electrolyte thickness	100 μm
Anode thickness	100 μm
<i>Thickness for anode-supported SOEC</i>	
Cathode thickness	100 μm
Electrolyte thickness	100 μm
Anode thickness	400 μm
<i>Thickness for electrolyte-supported SOEC</i>	
Cathode thickness	100 μm
Electrolyte thickness	400 μm
Anode thickness	100 μm

Mass, momentum, and energy conservations are the governing equations in Equations 4-8 [16].

$$\frac{\partial(\rho U)}{\partial x} + \frac{\partial(\rho V)}{\partial y} = S_m \quad (4)$$

$$\frac{\partial(\rho U U)}{\partial x} + \frac{\partial(\rho V U)}{\partial y} = -\frac{\partial P}{\partial x} + \frac{\partial}{\partial x} \left( \mu \frac{\partial U}{\partial x} \right) + \frac{\partial}{\partial y} \left( \mu \frac{\partial U}{\partial y} \right) + S_x \quad (5)$$

$$\frac{\partial(\rho U V)}{\partial x} + \frac{\partial(\rho V V)}{\partial y} = -\frac{\partial P}{\partial y} + \frac{\partial}{\partial x} \left( \mu \frac{\partial V}{\partial x} \right) + \frac{\partial}{\partial y} \left( \mu \frac{\partial V}{\partial y} \right) + S_y \quad (6)$$

$$\frac{\partial(\rho c_p U T)}{\partial x} + \frac{\partial(\rho c_p V T)}{\partial y} = \frac{\partial}{\partial x} \left( k \frac{\partial T}{\partial x} \right) + \frac{\partial}{\partial y} \left( k \frac{\partial T}{\partial y} \right) + S_T \quad (7)$$

$$\frac{\partial(\rho U Y_i)}{\partial x} + \frac{\partial(\rho V Y_i)}{\partial y} = \frac{\partial}{\partial x} \left( \rho D_{i,m}^{eff} \frac{\partial Y_i}{\partial x} \right) + \frac{\partial}{\partial y} \left( \rho D_{i,m}^{eff} \frac{\partial Y_i}{\partial y} \right) + S_{sp} \quad (8)$$

U and V: The velocity components in the x and y directions

ρ: the density of the gas mixture

μ: the viscosity of the gas mixture

k: the thermal conductivity

$c_p$ : the heat capacity

$D_{i,m}^{eff}$ : the effective diffusion coefficients of species in the gas mixture

The voltage can be calculated as seen in Equation 9.

$$V = E + \eta_{act,a} + \eta_{act,c} + \eta_{ohmic} \quad (9)$$

In Equation 9, E is the equilibrium potential and can be calculated by Equations 10-11 for H<sub>2</sub>O and CO<sub>2</sub> electrolysis, respectively [17].

$$E_{H_2} = 1.253 - 0.00024516T + \frac{RT}{2F} \ln \left[ \frac{P_{H_2}^I (P_{O_2}^I)^{0.5}}{P_{H_2O}^I} \right] \quad (10)$$

$$E_{CO} = 1.46713 - 0.0004527T + \frac{RT}{2F} \ln \left[ \frac{P_{CO}^I (P_{O_2}^I)^{0.5}}{P_{CO_2}^I} \right] \quad (11)$$

P: Partial pressures at the electrolyte-electrode interface

R: Universal gas constant

F: Faraday constant

Activation overpotentials can be calculated as seen in Equations 12-13 [17].

$$\eta_{act,H_2,i} = \frac{RTJ_{H_2}}{n_{H_2}FJ_{H_2,i}^0} \quad (12)$$

$$\eta_{act,CO,i} = \frac{RTJ_{CO}}{n_{CO}FJ_{CO,i}^0} \quad (13)$$

$J_{H_2,i}^0$  and  $J_{CO,i}^0$ : Exchange current densities for electrolysis of H<sub>2</sub>O and CO<sub>2</sub>

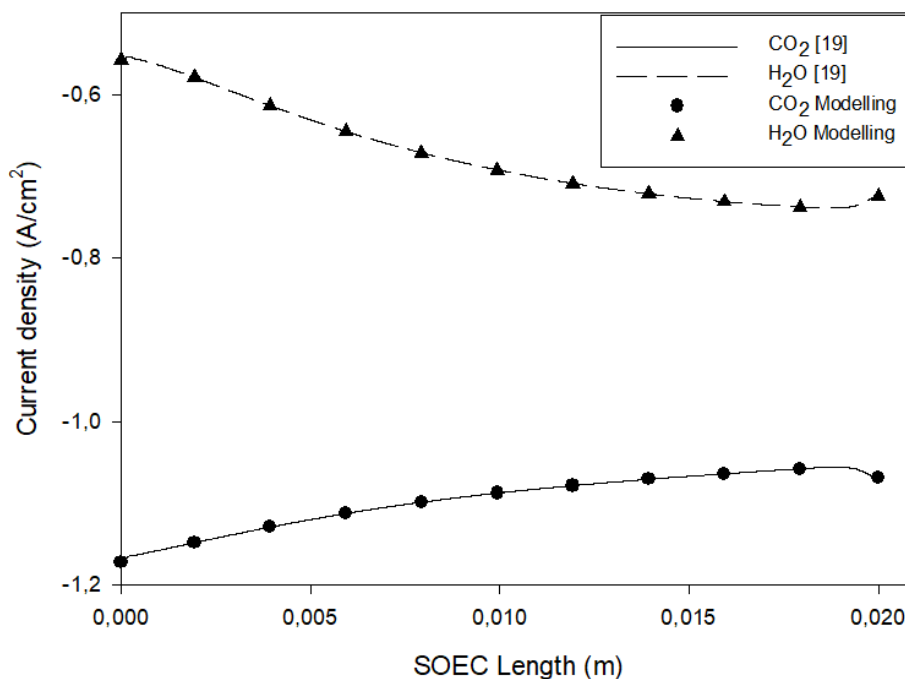
$n_{H_2}$  and: Number of electrons transferred per reaction

### 3. RESULTS AND DISCUSSIONS

The 2D SOEC model developed has been investigated numerically with COMSOL Multiphysics, Electrolyzers Module [18]. This module's electrolyte-supported, cathode-supported, and anode-supported models were formulated and examined under varying operational parameters.

### 3.1. Validation of the Mathematical Model

The validation of the 2D SOEC mathematical model is shown in Figure 2. In the validation study, the temperature was set at 1073 K, pressure at 1 bar, and the thickness of the anode, electrolyte, and cathode layers were taken as 100 μm, 100 μm, and 500 μm, respectively.

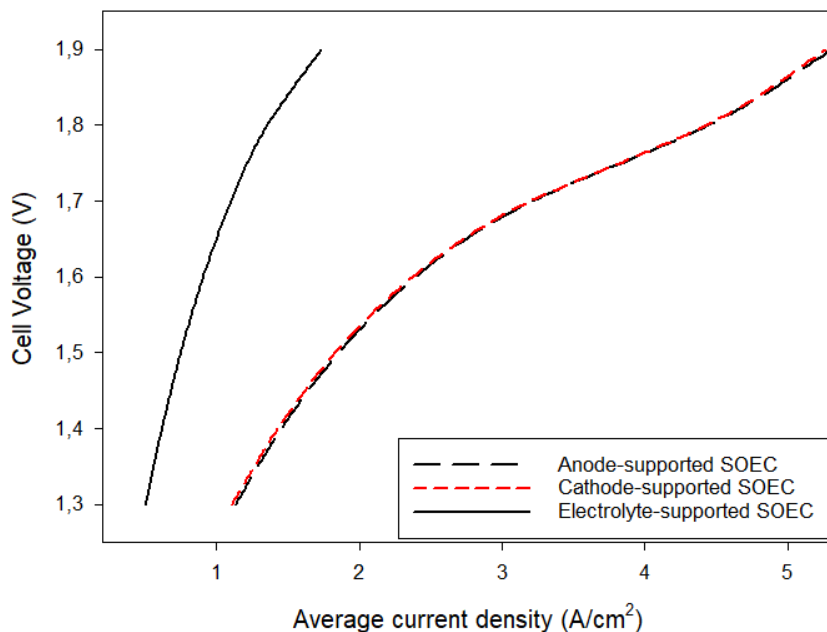


**Figure 2.** The validation of the 2D SOEC mathematical model [19]

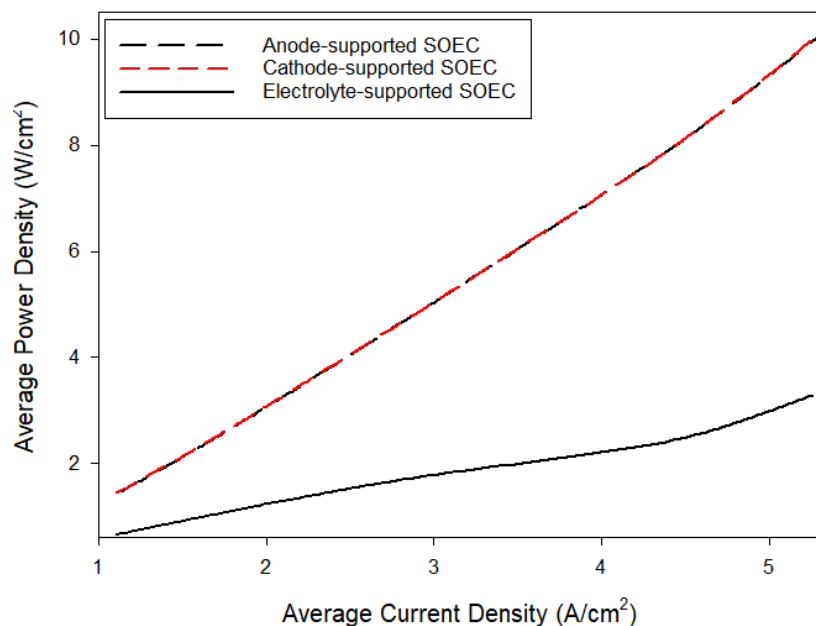
For validation purposes, the total cathodic current density was investigated for both H<sub>2</sub>O and CO<sub>2</sub> along the x-axis of the electrolyzer and compared. The study revealed a decrease in current density during the electrolysis of H<sub>2</sub>O, whereas an increase in current density was observed during CO<sub>2</sub> electrolysis. The results demonstrate a high degree of consistency for validation.

### 3.2. Supporting Layers Effect

SOECs can be classified based on the layers that play a supportive role in their structures. In this study, the performance of anode-supported, electrolyte-supported, and cathode-supported SOECs at a temperature of 1073 K was investigated. The polarization and power curves are shown in Figure 3 (a) and (b), respectively.



(a) Polarization Curve



(b) Power Curve

**Figure 3.** Polarization (a) and power (b) curves according to the supporting layer

As seen in Figures 3 (a) and 3 (b), the polarization and performance curves of anode-supported and cathode-supported SOECs are nearly identical. In the polarization curve, the average current density at 1.6 V is measured at approximately 2.3679 A/cm<sup>2</sup> for cathode-supported SOEC and approximately 2.3879 A/cm<sup>2</sup> for anode-supported SOEC. Similarly, at an average current density of approximately 5.30 A/cm<sup>2</sup>, cathode-supported SOEC generates 10 W/cm<sup>2</sup> average power



density, while this value is 10.1 W/cm<sup>2</sup> for anode-supported SOEC. Here, the determining factor is that the performance of electrolyte-supported SOECs remains significantly lower compared to other supporting types. The reason for this is the insufficient conductivity of the electrolyte layer and its increased thickness, which restricts the transport of electrons and ions.

Table 2 shows the mole fraction of H<sub>2</sub>O, H<sub>2</sub>, CO<sub>2</sub>, and CO in different supporting layers.

**Table 2.** Mole fraction of H<sub>2</sub>O, H<sub>2</sub>, CO<sub>2</sub> and CO in different supporting layer

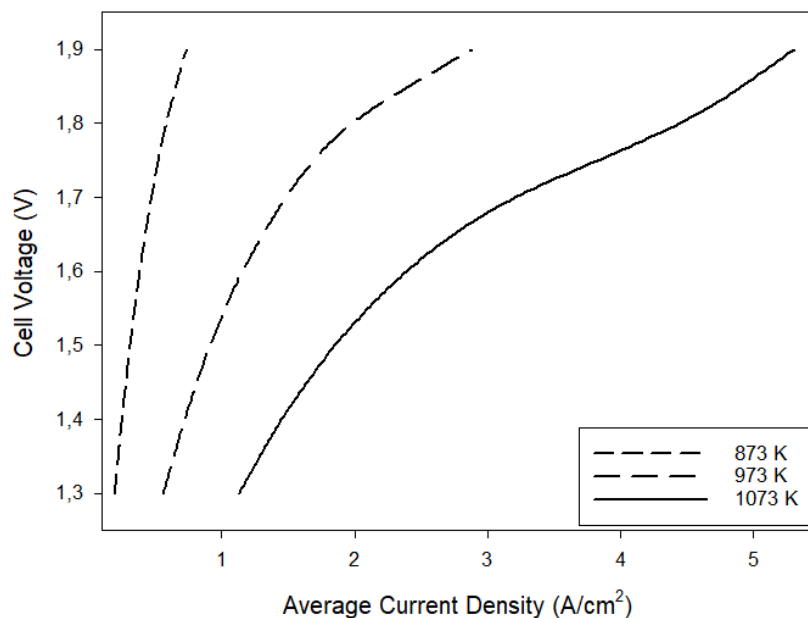
Mole Fraction	Anode-supported SOEC	Cathode-supported SOEC	Electrolyte-supported SOEC
H <sub>2</sub> O			
H <sub>2</sub>			
CO <sub>2</sub>			
CO			

For all three support layers, the consumption mole distributions of H<sub>2</sub>O and CO<sub>2</sub> occur as seen in Table 2, respectively in anode-supported, cathode-supported, and electrolyte-supported SOECs. This information is further corroborated when examining the mole distributions for H<sub>2</sub> and CO

formation, revealing that formation primarily occurs in anode-supported SOECs, followed by cathode-supported and electrolyte-supported SOECs, respectively. These mole distributions can also be cited as contributing factors to the performance curves.

### 3.3. Temperature Effects

When the effect of the support layer was examined, it was found in the previous section that the best performance for a SOEC occurred with an anode-supported SOEC. Therefore, in the subsequent analyses, considerations were made with the anode-supported SOEC. At different temperatures, the polarization curve of the anode-supported SOEC model is shown in Fig. 4.



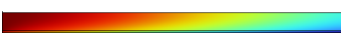
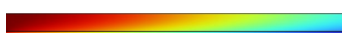
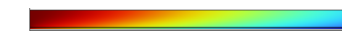

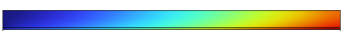
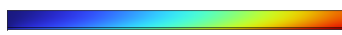

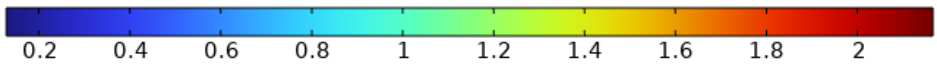


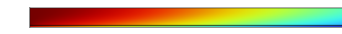




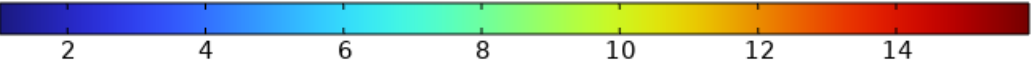
**Figure 4.** Polarization curve of the anode-supported SOEC model at different temperatures

Figure 4 shows the average current density versus cell voltage at different temperature operating conditions. As the temperature increases from 873 K to 1073 K, the average current density increases from 0.7378 A/cm<sup>2</sup> to 5.3047 A/cm<sup>2</sup>. An increase in temperature in a SOEC typically enhances polarization curves. This improvement stems from the fact that higher temperatures lead to more efficient chemical reactions within the cell. Electrochemical reactions accelerate proportionally with temperature, resulting in increased power generation in the SOEC. Moreover, elevated temperatures reduce the resistance between the electrode and electrolyte, thereby minimizing resistive losses and enabling higher power output at lower voltages. Temperature elevation also ameliorates the polarization curve by diminishing polarization losses, particularly

activation polarization, as reaction rates escalate. Consequently, temperature elevation contributes to the enhancement of both power and polarization curves in SOECs, promoting overall efficiency. However, it's essential to carefully determine the optimal operating temperature level to avoid compromising cell durability or material lifespan.

Table 3 shows the mole fraction of H<sub>2</sub>O, H<sub>2</sub>, CO<sub>2</sub>, and CO at different temperatures.

**Table 3.** Mole fraction of H<sub>2</sub>O, H<sub>2</sub>, CO<sub>2</sub> and CO at different temperatures

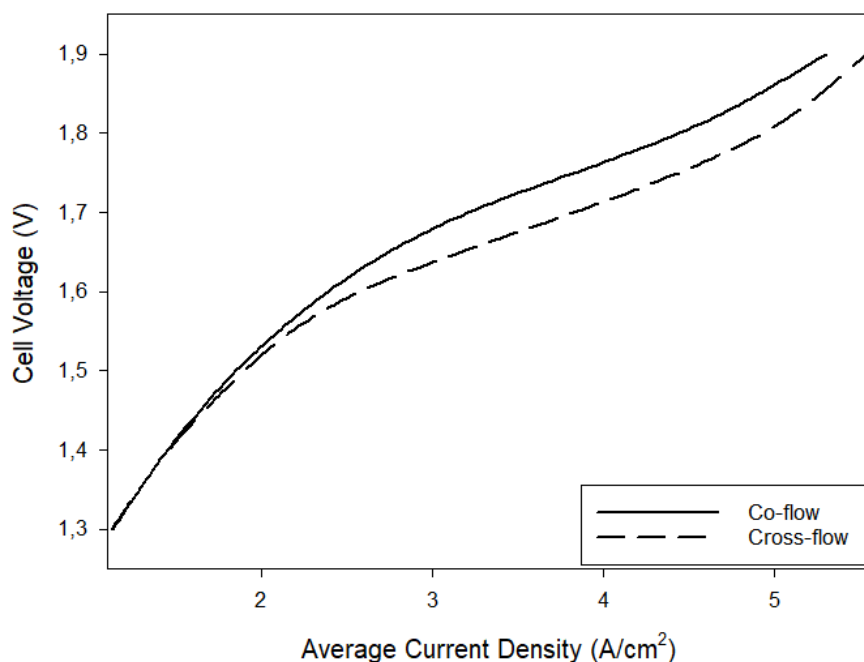
Mole Fraction	873 K	973 K	1073 K
H <sub>2</sub> O			
			
H <sub>2</sub>			
			
CO <sub>2</sub>			
			
CO			
			

As can be seen in Table 3, as temperature increases, certain changes occur in the molecular distribution of H<sub>2</sub>O and CO<sub>2</sub> electrolysis. With the temperature rise, the formation rates of H<sub>2</sub> and O<sub>2</sub> gases increase during H<sub>2</sub>O electrolysis. Higher temperatures facilitate easier dissociation of

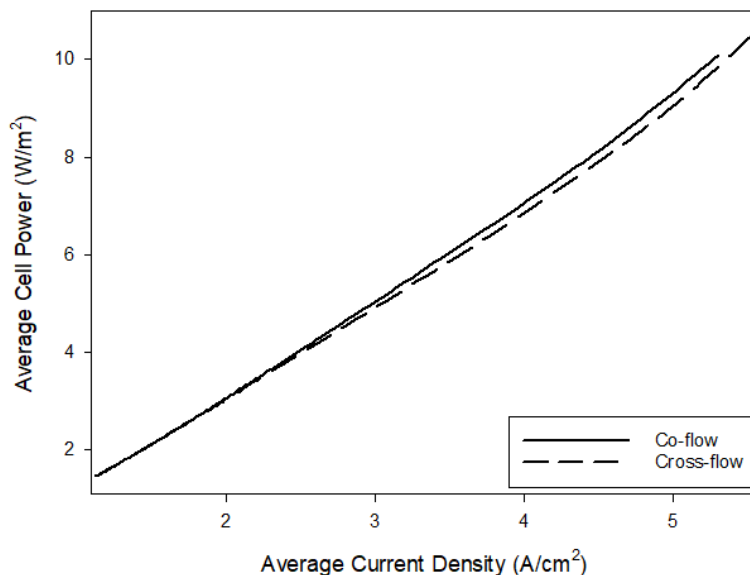
water molecules, thereby accelerating the electrolysis reactions. Temperature elevation in H<sub>2</sub>O electrolysis enables easier breakdown of H<sub>2</sub>O and production of more H<sub>2</sub> gases. During CO<sub>2</sub> electrolysis, the formation rates of CO gases increase with temperature. Elevated temperatures facilitate the breakdown of CO<sub>2</sub> molecules, increasing the formation rates of CO gases. Temperature elevation in CO<sub>2</sub> electrolysis leads to increased production of CO gases. So, as temperature increases, the formation rates of hydrogen, carbon monoxide, and oxygen gases increase in both H<sub>2</sub>O and CO<sub>2</sub> electrolysis. This implies that higher temperatures can enhance electrolysis efficiency.

### 3.4. Flow Direction Effects

The previous sections of the analysis were conducted under the assumption that the gases entering the anode and cathode layers were flowing in the same direction. In this section, the effects of both co-flow and counter-flow configurations on the performance are examined in a 1073 K anode-supported SOEC. The polarization and power curves of the co-flow and cross-flow anode-supported SOEC model are shown in Figure 5.



(a) Polarization Curve



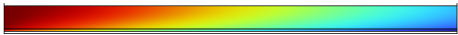

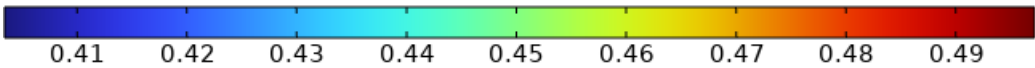


(b) Power Curve

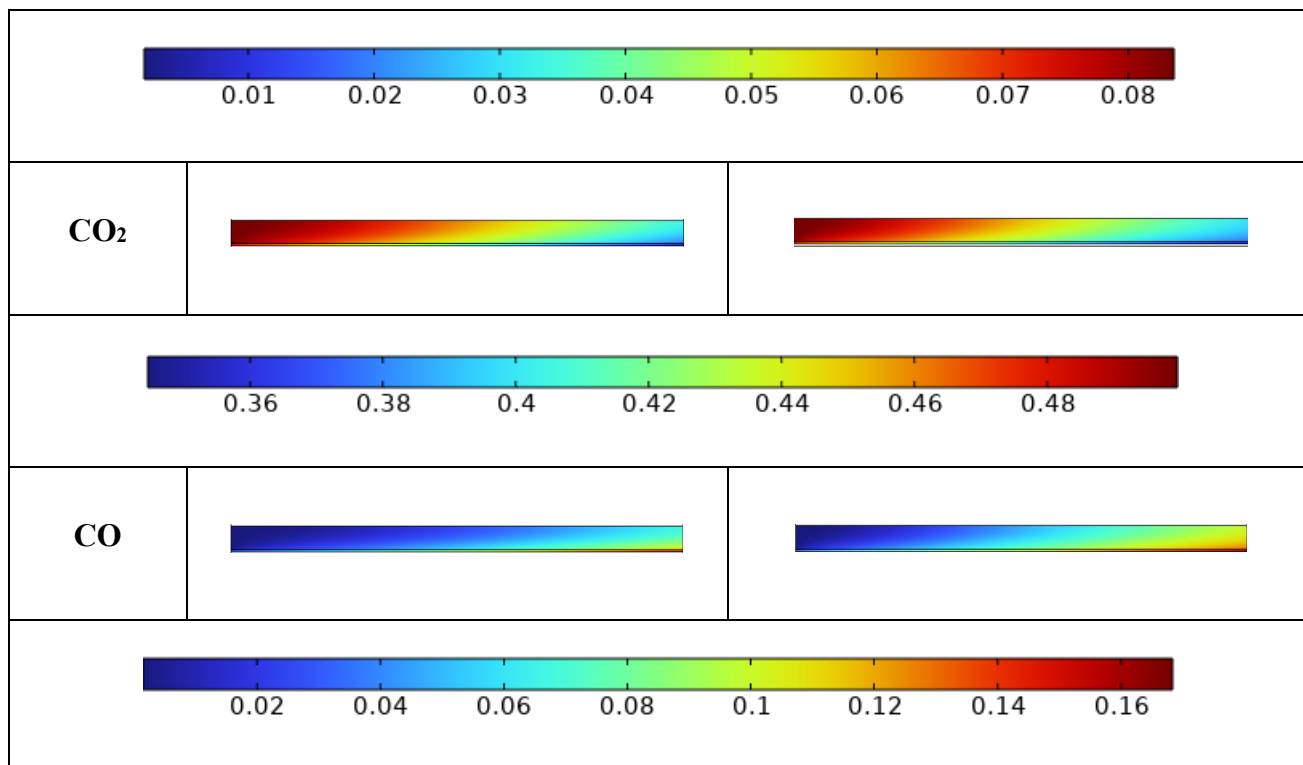
**Figure 5.** Polarization (a) and power (b) curves of the co-flow and cross-flow model

As seen in Figures 5 (a) and 5 (b), polarization and performance curves of co-flow and cross-flow SOECs are nearly identical. In the polarization curve, the average current density at 1.6 V is measured at approximately 2.3879 A/cm<sup>2</sup> for co-flow SOEC and approximately 2.5704 A/cm<sup>2</sup> for cross-flow SOEC. Similarly, at an average current density of approximately 3.20 A/cm<sup>2</sup>, co-flow SOEC generates 5.4515 W/cm<sup>2</sup> average power density, while this value is 6.4994 W/cm<sup>2</sup> for cross-flow SOEC.

Table 4 shows the mole fraction of H<sub>2</sub>O, H<sub>2</sub>, CO<sub>2</sub>, and CO at co-flow and cross-flow.

**Table 4.** Mole fraction of H<sub>2</sub>O, H<sub>2</sub>, CO<sub>2</sub> and CO at co-flow and cross flow

Mole Fraction	Co-flow	Cross-flow
H <sub>2</sub> O		
		
H <sub>2</sub>		



As can be seen in Table 4, in anode-supported SOECs, the performance of co-flow and counter-flow configurations can be elucidated. Co-flow, where both gases move in the same direction within the cell, promotes homogeneous temperature and pressure distributions, facilitating efficient gas mixing and diffusion, thus enhancing electrochemical reaction rates. This configuration often leads to stable and balanced cell operation. Conversely, in counter-flow, where gases move in opposite directions, distinct temperature and pressure conditions may arise, with higher temperature and lower pressure typically observed at the anode and cathode. This arrangement may reduce gas mixing and diffusion, potentially influencing electrochemical reaction rates and overall performance, as different gases need to be generated and react under varying conditions. Thus, while co-flow generally ensures homogeneous operation and improved performance, counter-flow may introduce heterogeneity and affect performance depending on specific application and design requirements.

#### 4. CONCLUSION

In this study, a 2D SOEC model was investigated to determine the performance of CO<sub>2</sub> and H<sub>2</sub>O co-electrolysis. Firstly, the numerical results were validated with a different study, and it was observed that the results were highly consistent.

The polarization and performance curves of anode-supported and cathode-supported SOECs exhibited close resemblance. At 1.6 V, the average current density for cathode-supported SOEC was approximately 2.3679 A/cm<sup>2</sup>, slightly lower than that of anode-supported SOEC, which was approximately 2.3879 A/cm<sup>2</sup>. Moreover, at an average current density of around 5.30 A/cm<sup>2</sup>, the cathode-supported SOEC yielded an average power density of 10 W/cm<sup>2</sup>, while the anode-supported SOEC achieved 10.1 W/cm<sup>2</sup>. However, electrolyte-supported SOECs exhibited significantly lower performance attributed to the inadequate conductivity and increased thickness of the electrolyte layer, hindering electron and ion transport. Furthermore, the consumption mole distributions of H<sub>2</sub>O and CO<sub>2</sub> differed across the support types, with anode-supported SOECs showing the highest formation of H<sub>2</sub> and CO, followed by cathode-supported and electrolyte-supported SOECs. These findings underscored the influence of support type on the performance characteristics of SOECs.

Increasing temperature in SOECs leads to higher average current densities and enhanced polarization curves. This improvement was attributed to more efficient chemical reactions at elevated temperatures, which accelerated electrochemical reactions and reduced resistance between electrodes and electrolyte interfaces, consequently minimizing resistive losses and enabling higher power output at lower voltages. Additionally, temperature elevation decreased both activation and ohmic polarization, further enhancing overall efficiency. Furthermore, as the temperature rose, there were notable changes in the molecular distribution during the electrolysis of H<sub>2</sub>O and CO<sub>2</sub>, resulting in increased formation rates of H<sub>2</sub>, CO, and O<sub>2</sub> gases. These findings suggested that higher temperatures can significantly improve electrolysis efficiency by facilitating easier dissociation of water and CO<sub>2</sub> molecules and increasing gas production rates. However, careful consideration of the optimal operating temperature is crucial to maintain cell durability and material lifespan.

Polarization and performance curves of co-flow and cross-flow SOECs exhibited minor differences, with co-flow demonstrating slightly lower average current density but comparable power density at 1.6 V compared to cross-flow. In anode-supported SOECs, co-flow configuration promoted homogeneous temperature and pressure distributions, facilitating efficient gas mixing and diffusion, thus enhancing electrochemical reaction rates and ensuring stable cell operation. Conversely, counter-flow configuration may lead to distinct temperature and pressure conditions, potentially reducing gas mixing and diffusion and affecting overall performance. While co-flow

generally results in improved performance due to its homogeneous operation, the choice between co-flow and counter-flow configurations should consider specific application and design requirements.

### **ACKNOWLEDGMENT**

The author gratefully acknowledges Nigde Omer Halisdemir University for allowing to use of software and computer facilities.

### **DECLARATION OF ETHICAL STANDARDS**

The author of the paper submitted declares that nothing necessary for achieving the paper requires ethical committee and/or legal-special permissions.

### **CONTRIBUTION OF THE AUTHORS**

**Berre Kumuk:** Performed numerical analysis and analyse the results. Wrote the manuscript

### **CONFLICT OF INTEREST**

There is no conflict of interest in this study.

### **REFERENCES**

- [1] Gómez SY, Hotza D. Current developments in reversible solid oxide fuel cells. *Renewable and Sustainable Energy Reviews* 2016;61:155–174.
- [2] Li Z, Zhang H, Xu H, Xuan J. Advancing the multiscale understanding on solid oxide electrolysis cells via modelling approaches: A review. *Renewable and Sustainable Energy Reviews* 2021;141:110863.
- [3] Tucker MC. Progress in metal-supported solid oxide electrolysis cells: A review. *International Journal of Hydrogen Energy* 2020;45:24203–24218.
- [4] Laguna-Bercero MA. Recent advances in high temperature electrolysis using solid oxide fuel cells: A review. *Journal of Power Sources* 2012;203:4–16.
- [5] Ni M, Leung MKH, Leung DYC. Technological development of hydrogen production by solid oxide electrolyzer cell (SOEC). *International Journal of Hydrogen Energy* 2008;33:2337–2354.
- [6] Lahrichi A, El Issmaeli Y, Kalanur SS, Pollet BG. Advancements, strategies, and prospects of solid oxide electrolysis cells (SOECs): Towards enhanced performance and large-scale sustainable hydrogen production. *Journal of Energy Chemistry* 2024;94:688–715.



- [7] Kamkeng ADN, Wang M, Hu J, Du W, Qian F. Transformation technologies for CO<sub>2</sub> utilisation: Current status, challenges and prospects. *Chemical Engineering Journal* 2021;409:128138.
- [8] Zheng Y, Chen Z, Zhang J. Solid Oxide Electrolysis of H<sub>2</sub>O and CO<sub>2</sub> to Produce Hydrogen and Low-Carbon Fuels. *Electrochemical Energy Reviews* 2021;4:508–517.
- [9] Ramdin M, De Mot B, Morrison ART, Breugelmans T, Van Den Broeke LJP, Trusler JPM, et al. Electroreduction of CO<sub>2</sub>/CO to C<sub>2</sub> Products: Process Modeling, Downstream Separation, System Integration, and Economic Analysis. *Industrial and Engineering Chemistry Research* 2021;60:17862–17880.
- [10] Song Y, Zhang X, Xie K, Wang G, Bao X. High-Temperature CO<sub>2</sub> Electrolysis in Solid Oxide Electrolysis Cells: Developments, Challenges, and Prospects. *Advanced Materials* 2019;31:1–18.
- [11] Xu H, Chen B, Irvine J, Ni M. Modeling of CH<sub>4</sub>-assisted SOEC for H<sub>2</sub>O/CO<sub>2</sub> co-electrolysis. *International Journal of Hydrogen Energy* 2016;41:21839–21849.
- [12] Song Y, Zhou Z, Zhang X, Zhou Y, Gong H, Lv H, Liu Q, Wang G, Bao X. Pure CO<sub>2</sub> electrolysis over a Ni/YSZ cathode in a solid oxide electrolysis cell. *Journal of Materials Chemistry A* 2018;6:13661–13667.
- [13] Wang Y, Banerjee A, Deutschmann O. Dynamic behavior and control strategy study of CO<sub>2</sub>/H<sub>2</sub>O co-electrolysis in solid oxide electrolysis cells. *Journal of Power Sources* 2019;412:255–264.
- [14] Luo Y, Shi Y, Chen Y, Li W, Jiang L, Cai N. Pressurized tubular solid oxide H<sub>2</sub>O/CO<sub>2</sub> electrolysis cell for direct power-to-methane. *AIChE Journal* 2020;66:1–14.
- [15] Mahmood A, Bano S, Yu JH, Lee KH. Performance evaluation of SOEC for CO<sub>2</sub>/H<sub>2</sub>O co-electrolysis: Considering the effect of cathode thickness. *Journal of CO<sub>2</sub> Utilization* 2019;33:114–120.
- [16] Ni M. Computational fluid dynamics modeling of a solid oxide electrolyzer cell for hydrogen production. *International Journal of Hydrogen Energy* 2009;34:7795–7806.
- [17] Ni M. Modeling of SOFC running on partially pre-reformed gas mixture. *International Journal of Hydrogen Energy* 2012;37:1731–1745.
- [18] COMSOL Multiphysics. *The COMSOL Multiphysics Reference Manual*. Manual 2015:1–1336.
- [19] Ni M. 2D thermal modeling of a solid oxide electrolyzer cell (SOEC) for syngas production by H<sub>2</sub>O/CO<sub>2</sub> co-electrolysis. *International Journal of Hydrogen Energy* 2012;37:6389–6399.